Front. Chem. China 2009, 4(2): 160–167
DOI 10.1007/s11458-009-0029-4

RESEARCH ARTICLE

Lina YU, Dongfeng WANG, Weisheng HU, Haiyan LI, Minmin TANG

Study on the preparation and adsorption thermodynamics of chitosan microsphere resins

Abstract The aim of this research is to study the thermodynamic behavior of resins of chitosan microspheres (RCM) in adsorbing Cu^{2+}, so that the theoretical basis of the application of RCM to eliminate metal ions in wastewater or fruit and vegetable juice can be obtained. First, RCM were prepared from chitosan as a raw material by using reverse phase suspension cross-linking polymerization, and some physicochemical properties of RCM were characterized. Second, the adsorption behavior of Cu^{2+} onto RCM was investigated by the batch method. The results show that the diameter of the microspheres was relatively uniform and the surface of microspheres was compacted with pores. The physical properties of the RCM were as follows: water content 51.982%, skeletal density 1.212 $g \cdot cm^{-3}$, pileup density 0.862 $g \cdot mL^{-1}$, porosity was in 0.554 and crosslinking degree was in 13.581%. The saturated adsorption capacity of RCM for Cu^{2+} was 0.993 $mmol \cdot g^{-1}$. At the same time, the results also indicated that the adsorption of RCM for Cu^{2+} followed the Langmuir isotherm equation: $C_e/Q = 11.614 + 1.0075C_e$ at 313 K and the adsorption appeared to be of the monomolecular type. The adsorption was found through thermodynamic study to be a spontaneous endothermic process of increased entropy. The adsorption potential decreased gradually as Cu^{2+} concentration increased at the same temperature and it increased as temperature increased at the same initial concentration of Cu^{2+}.

Keywords resins of chitosan microspheres, adsorption Cu^{2+}, isothermal curve, thermodynamics

Translated from *Periodical of Ocean University of China*, 2008, 38(1) (in Chinese)

Lina YU, Dongfeng WANG (✉), Weisheng HU, Haiyan LI, Minmin TANG
College of Food Science and Technology, Ocean University of China, Qingdao 266003, China
E-mail: wangdf@ouc.edu.cn

Lina YU
Shandong Peanut Research Institute, Qingdao 266100, China

1 Introduction

At present, heavy metal pollution sources in the natural environment has gained much concern because of more and more heavy metals being released into water bodies and becoming harmful to humans. For example, copper at relatively high doses could accumulated in the liver. In addition, even minute quantities of copper existing in the water bodies might produce toxicity to various aquatic species. A few techniques can eliminate the harmful metallic ions from aqueous solution, such as the ion exchange method, the reverse osmosis process, the adsorption method, the chelating capacity and the precipitation method. Among these, the adsorption method is the most effective and widely used technology [1–3]. Compared with the other technologies, activated carbon and chelating ion exchanger resin used in water treatment and the three wastes industry have become more and more popular methods. However, activated carbon and commercial chelating resin material are expensive. Therefore, the low cost substitute has become the focus of present researches in this field. Both the biological adsorption method [4] and the adsorption by using biomaterials [5] are considered to be the emerging technologies for treating waste water containing heavy metals.

Chitosan is a kind of biopolymer obtained by deactivated chitin and is composed mainly of β-(1-4)-2-amino-2-deoxy-D-glucopyranose and β-(1-4)-2-acetamido-2-deoxy-D-glucopyranose repeating units. The content of β-(1-4)-2-amino-2-deoxy-D-glucopyranose is more than 60%. Chitosan is considered to be the natural polymer for recycling heavy metals, because the C-2 amino group nitrogen atom or the C-6 hydroxyl group oxygen atom of chitosan can provide isolated electron pairs to metal ions and the coordination effect happens between chitosan and metal ions [6]. Unfortunately, in an acidic solution, chitosan can be protonated and dissolved in the acidic medium due to its free amino groups. Therefore, physical or chemical modification is needed to increase the sorption properties and prevent chitosan from dissolving in acidic solution [7–9]. Cross-linking can change the crystalline

nature of chitosan and enhance the resistance of chitosan against acid, alkali and chemicals. This study was designed to investigate the adsorption thermodynamics of resins of chitosan microspheres (RCM). The RCM was prepared by the reversed phase suspension cross-linking polymerization and the structure and the thermal stability of RCM was analyzed in this study. At the same time, the thermodynamic behavior of RCM adsorption Cu^{2+} was proposed for the first time and it will provide theoretical basis for the application of RCM on the wastewater treatment and fruit vegetable juice clarification process.

2 Experimental

2.1 Material and instruments

Chitosan, with a percent degree of deacetylation (DD%) of 85.3 (Manufacturer's data), was provided by the Lizhong Chitosan Company Limited, China, and used without any purification. Liquid paraffin and acetic ester were analytical reagents produced by Sinopharm Chemical Reagent Co., Ltd. China. All other reagents were of analytical grade and used as received.

The instruments used are as follows, Scanning electron microscope (SEM) (JSM-840), JEOL Ltd. Differential scanning calorimetry (DSC) (200F3), NETZSCH-Gerätebau GmbH. Fourier Transform Infrared Spectroscopic (NEXUE 470 FT-IR), Nicolet. X-ray power diffraction (Rigaku D/MAX 2500), Rigaku Corporation Japan. Ultraviolet-visible spectrophotometer (UV-2102 PC), Unico (Shanghai) Instrument Co., Ltd.

2.2 Preparation of RCM

The RCM was prepared by using the reversed phase suspension cross-linking polymerization according to the patent [10] and it was modified slightly. The main preparation process of the RCM is as follows: The chitosan acetic acid solution was added to liquid paraffin. Then, the emulsifier and the pore-foaming agent were added to the above mixture with stirring for 20 min. The reaction mixture was stirred continuously for 3 h after the cross-linking agent glutaraldehyde was added. The RCM were rinsed with petroleum ether, acetone, ethanol and distilled water in turn. The particles were dried in vacuum condition by DZX-6 vacuum drying oven (50°C) for around 48 h and stored at room temperature.

2.3 Description of RCM physical properties [11]

2.3.1 Cross-linking degree ζ

The 0.25 g (W_1) RCM was immersed in 2.0% (V/V) acetic acid solution for 24 h. Then, the RCM was dried in the dryer at 105°C for 4 h and weighed (W_2). And the cross-linking degree can be calculated by the following formula: $\zeta(\%) = (W_1 - W_2)/W_1 \times 100$.

2.3.2 Water content H

The 0.1 g RCM swelled adequately in distilled water, and was filtered and weighed (G_1) after superficially drying. Then, the RCM was dried in the dryer at 105°C for 4 h and weighed (G_2). The water content can be calculated by the following formula: $H(\%) = (G_1 - G_2)/G_1 \times 100$.

2.3.3 Pileup density ρ_P

The pileup density refers to the RCM quantity of unit volume including the skeletal volume and the porosity volume of microspheres and the interstitial volume between microspheres. The 2.0 mL (V_P) RCM was added to the 10.0 mL measuring cylinder and weighed the RCM quantity (W). Then, the pileup density can be calculated by the following formula: ρ_P ($g \cdot mL^{-1}$) = W/V_P.

2.3.4 Skeletal density ρ_T

The 5.0 mL *n*-heptane was added to the 10.0 mL measuring cylinder and spilled over after weighing (W_1). The 0.1 g (W) RCM and 2.0 mL *n*-heptane were added to the measuring cylinder and the quantity (W_2) will be obtained when enough 5.0 mL *n*-heptane was added to after standing for 2 h. The skeletal volume and the skeletal density can be calculated by the following formulas, respectively: $V_T = (W_1 - W_2 + W)/dt$ ($dt = 0.6830$, the n-heptane density $g \cdot cm^{-3}$), ρ_T ($g \cdot cm^{-3}$) = W/V_T.

2.3.5 Porosity degree P

The porosity degree can be calculated by the following formula: $P = \rho_T H/(\rho_T H + 1 - H)$ (ρ_T is the skeletal density, $g \cdot cm^{-3}$, H is the water content, %).

2.4 Characterization

The morphological characteristic of RCM was carried out by SEM. The FTIR was conducted using the NEXUE 470 FTIR Nicolet (Wavenumber range 4000–400 cm^{-1}). The sample was prepared by the KBr pellet method. The X-ray powder diffraction (XRD) data were measured using a Rigaku D/MAX 2500 XRD. The scanning speed was $2°/min^{-1}$ with Kα and the scanning angle was from 5° to 50°. The DSC of the samples was performed using Netzsch, Model 200F3 DSC (Temperature range 25°–400°C). The heating rate was 10°C min^{-1} and the cooling gas was nitrogen 20 $mL \cdot min^{-1}$.

2.5 Measurement of adsorption capacity

The 0.1 g of RCM was swelled by distilled water and it was put into the 100.0 mL conical flask when the water was

removed from RCM by using vacuum infiltration. Then, the 10.0 mL $CuSO_4$ solution was added to the flask and the mixture was oscillated for 24 hours at a certain temperature. Finally, the absorbance of the reaction solution was determined using the Unico 2102 PC UV-Vis spectrophotometer at 700 nm. The adsorption capacity can be calculated by the following formula: $Q=(C_0-C)V/W$ where Q ($mmol\cdot g^{-1}$) is the adsorption capacity, C_0 ($mmol\cdot L^{-1}$) is the $CuSO_4$ solution concentration before adsorption, C ($mmol\cdot L^{-1}$) is the $CuSO_4$ solution concentration after adsorption, V (L) is the reaction solution volume and W (g) is the quantity of RCM.

2.6 Measurement of adsorption isotherm

The adsorption effect on 10.0 mL $CuSO_4$ solutions of varying concentration (10.0 to 100.0 $mmol\cdot L^{-1}$) by 0.1 g RCM was carried out at temperature 30, 40 and 50°C for oscillating 24 h. When the reaction was over, the absorbance of the reaction solution was measured at 700 nm and the equilibrium adsorption capacity was calculated according to the formula in 1.5. Then, the evaluation on the influencing factors and thermodynamic properties of adsorption effect on $CuSO_4$ by RCM can be conducted.

3 Results and discussion

3.1 Physical properties and morphological characteristic of RCM

3.1.1 Physical properties of RCM

The preparation of RCM used reversed phase suspension cross-linking polymerization. RCM was a type of light yellow spherical resin with smooth surface observed by SEM (Fig. 1) and the average particle diameter of RCM was about 500 μm. Under this experimental condition, such as chitosan with 85.3% deacetylation (DD%) and molecular weight 5.9×10^5 determined by viscosity-average, stirring speed 350 $rmin^{-1}$ and the reaction solution with pH 7.5, the particle distribution of RCM was found to be uniform and it was tight and porous on the RCM surface. The physical properties of RCM are listed in Table 1, which shows that the RCM has porous, cross-linking and hygroscopic capacity. The RCM has certain stereo conformation and rigidity features because of the skeletal structure coming from cross-linking property. The pores can provide the conditions for the adsorption of water and metal ions onto RCM. Meanwhile, the RCM cannot be excessive water swelling and the stereo conformation of RCM might not be damaged due to the cross-linking property.

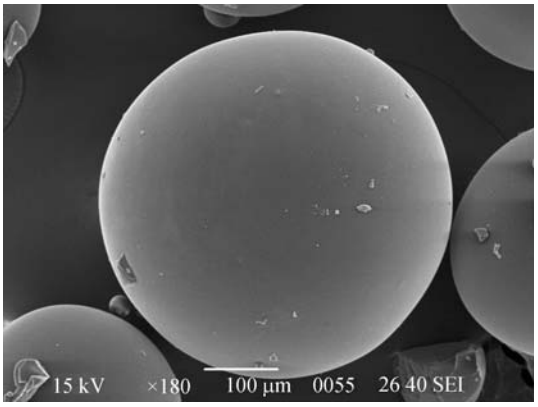

Fig. 1 SEM picture of RCM

3.1.2 FTIR spectroscopy of RCM

The FTIR spectra of RCM and chitosan powder are shown in Fig. 2. The overlapping peak consisted of ν(O—H) and ν(N—H) is at 3444.86 cm^{-1} and the ν(—CH_3) and ν(—CH_2) appeared at 2917.82 and 2875.65 cm^{-1}, respectively, in chitosan powder. The characteristic absorption peak of amino group δ(—NH_2) was at 1597.87 cm^{-1}. In addition, the three characteristic absorption peaks of amide (N—H—C═O) appeared in the spectra because of a certain amount of acetyl amino groups existing in the chitosan molecule [12]. They were amide I 1649.84 cm^{-1} (ν (C═O)), amide II 1540.99 cm^{-1} (δ(N—H) and ν (C—N)) and amide III 1321.45 cm^{-1} (ν(C—N) and δ (N—H)), respectively. The δ (—CH_2) and δ(—CH_3) were at 1420.78 cm^{-1} and 1380.68 cm^{-1}, respectively. The δ (O—H) belonging to chitosan C_3—OH appeared at 1259.77 cm^{-1}, the glycosidic bond ν(C—O—C) was at 1154.60 cm^{-1}, the polysaccharide ν(C—OH) was at 1087.55 cm^{-1} and the characteristic absorption peak of β-D-glucopyranoside was at 897.47 cm^{-1}. In the RCM FTIR spectrum, the ν(O—H) and ν(N—H) overlapping peak shifted to low wave number from 3444.86 cm^{-1} to near 3420.21 cm^{-1}, the ν(—CH_3) shifts to high wave number 2925.88 cm^{-1} and its absorbance intensity increased, and the position of ν(—CH_2) was almost unchangeable. The amide I shifted to high wave number 1715.07 cm^{-1} and it was found that the bending adsorption peak of —NH_2 near 1650 cm^{-1} and amide II disappeared and the characteristic adsorption peak of Schiff base ν(C═N) appeared at 1573.36 cm^{-1}. The results suggested that amino group and partly acetyl amino group

Table 1 Physical properties of RCM

Water content H/%	Cross-linking degree ζ/%	Pileup density ρ_P/($g\cdot mL^{-1}$)	Skeletal density ρ_T/($g\cdot cm^{-3}$)	Porosity degree P
51.982±1.944	13.581±0.677	0.862±0.007	1.212±0.453	0.554±0.097

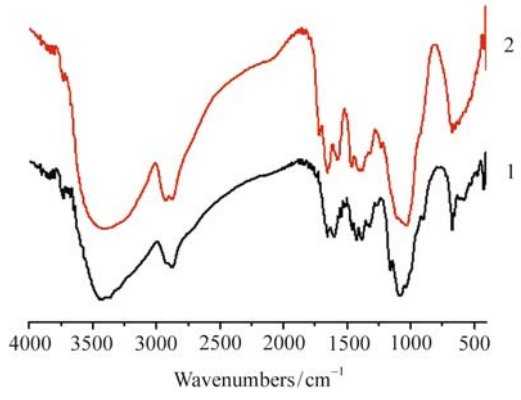

Fig. 2 FTIR spectra of chitosan powder (1) and RCM (2)

participated in the cross-linking reaction to be C = N bond. The amide III, δ(–CH_2), δ(–CH_3), δ(O–H) in C_3–OH and v (C–OH) shifted to the low wave numbers 1317.34, 1400.20, 1376.04, 1227.50 and 1031.00 cm^{-1}, respectively. The v(C–O–C) and β-D-glucopyranoside intensity were reduced after the cross-linking reaction. The possible reason of that is the long chitosan chain may have taken a coiling and curling spatial structure and the formation of hydrogen bond between primary alcoholic hydroxyl and nitrogen or hydrogen atom can be carried out. The ring opening reaction of β-D-glucopyranose has not occurred during the process of cross-linking reaction because the formation of hydrogen bond between amino group and hydroxyl group strengthened the force of glucose units in chitosan.

3.1.3 XRD analysis of RCM

Chitosan has good crystalline and strong hydrogen bonding between molecules because of the hydroxyl groups and free amino groups. The XRD spectrum of chitosan shows that chitosan had two different crystal morphologies, Form I (2θ is at near 10°) and Form II (2θ is at near 20°), which belong to the monoclinic system [13]. On the preparation process, the strong hydrogen bonding among molecules and molecule chain regularity might be destroyed, because chitosan can react with acetic acid and be cross-linked. At the same time, the polymer molecular activity ability will be limited, and thus cause the crystallization capacity of polymer to decrease. To compare with the XRD spectrum of chitosan powder, the 10° diffraction peak disappeared completely, the 20° diffraction peak relative intensity decreased significantly and the amorphous area relative increased. The results indicated that the RCM crystalline degree decreased and the cross-linking product was generated.

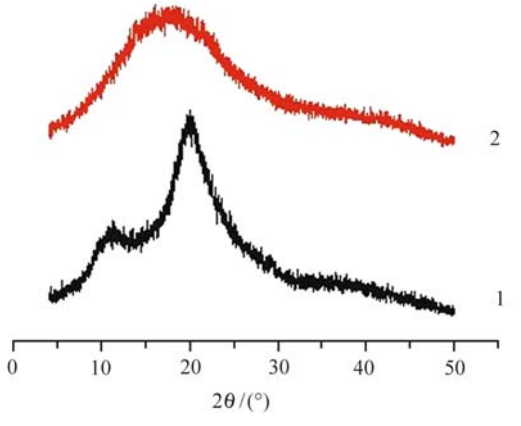

Fig. 3 XRD spectra of chitosan powder (1) and RCM (2)

3.1.4 Differential scanning calorimetry (DSC) analysis of RCM

The DSC curves for RCM and chitosan powder are shown in Fig. 4. The DSC curves contained two heating stages, the first heating stage was from 25°C to 200°C and the second heating stage was from 200°C to 400°C. In the first heating stage, the initial point was 57.06°C, the terminal point was 82.88°C and the endothermic enthalpy ΔH was 40.49 J·g^{-1} in the endothermic peak of chitosan powder. The experimental data of RCM were 39.93°C, 87.74°C and 63.41 J·g^{-1}, respectively. The maximum of endothermic peak and the endothermic enthalpy in RCM was higher than that of chitosan powder. Generally, polysaccharide molecules have stronger affinity to water and easily combine with water. Two kinds of polar bonds, hydroxyl group and amino groups, exist in the chitosan molecular structure and they can form intra-molecular hydrogen bond between chitosan and water, which become the chitosan crystal water. The binding ability of hydroxyl group with water will be higher than that of amino group. Furthermore, the energy required to breakdown hydrogen bond formed from hydroxyl group and water also was higher than that of from amino group and water. The endothermic peak was mostly caused by the dehydration of chitosan macromolecule [14]. The endothermic peak of chitosan powder shows that a considerable amount of water molecules was released when the temperatures were

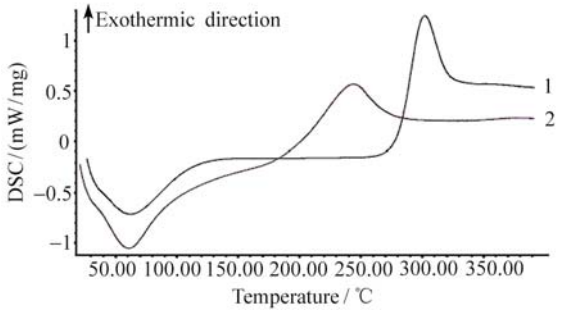

Fig. 4 DSC spectra of chitosan powder (1) and RCM (2)

below 100°C. Therefore, it can be considered that water molecules mainly combine with amino groups in chitosan. Hydrogen bonds mostly existed between amino group and the water molecules in chitosan powder, so it would only need low energy to break those bonds. However, some amino groups of chitosan would react with glutaraldehyde to form a Schiff base, after chitosan was prepared cross-linking spherical resins. Thus, some new hydrogen bonds would be produced between hydroxyl groups and water molecules, which combined with amino groups initially, and the rupture of those hydrogen bonds will require more energy. Therefore, the endothermic enthalpy of RCM was higher than that of chitosan powder.

In the second heating stage, the initial point was 288.58°C, the terminal point was 326.09°C and the exothermic enthalpy was 124.2 $J \cdot g^{-1}$ in the exothermic peak of chitosan powder. The experimental data in RCM was 215.36°C, 276.68°C and 85.63 $J \cdot g^{-1}$, respectively. The exothermic peak maybe related to the thermal and oxidative decomposition of chitosan, the volatilization and elimination of volatile products. The thermolysis of polysaccharide happened from the beginning of the random breakage in glycosidic bond. Then, acetic acid, butyrate and a series of fatty acids (2, 3 and 6 carbons are the chief species) can be formed with the thermal degradation going on [15]. The maximum of exothermic peak in RCM was lower than that of chitosan powder. When the preparation of cross-linking spherical resins was carried out, amino group would react with glutaraldehyde to form new covalent bond and to destroy the hydrogen bond of chitosan. Consequently, the crystalline and thermal stability of chitosan would decrease and RCM was less stable than chitosan powder under heating condition. The DSC curves show that the thermal degradation temperature and the exothermic enthalpy of RCM were lower than those of chitosan powder.

3.2 The adsorption capacity

Figure 5 shows the working curve of $CuSO_4$ and Fig. 6 shows the adsorption isotherms of Cu^{2+} onto RCM. The Langmuir isotherm adsorption model is suitable for describing the adsorption behavior of metal ions onto the surface of natural particles [16–18]. The usual Langmuir equation is $C_e/Q = 1/K_bQ_s + C_e/Q_s$, in which C_e is the adsorption equilibrium concentration (mmol·L^{-1}), Q is equilibrium adsorption capacity (mmol·g^{-1}), Q_s is monolayer saturated adsorption capacity of resins (mmol·g^{-1}) and K_b is Langmuir constant ($L \cdot mmol^{-1}$). Linear fitting to the adsorption capacity-temperature curve was carried out with the Langmuir isotherm adsorption model, and the fitting results are shown in Fig. 7 and Table 2.

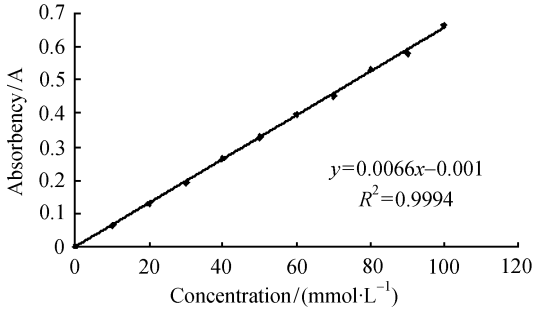

Fig. 5 Working curve of $CuSO_4$

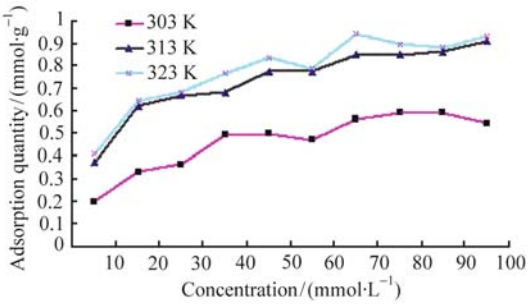

Fig. 6 Adsorption isotherms of Cu^{2+} onto RCM

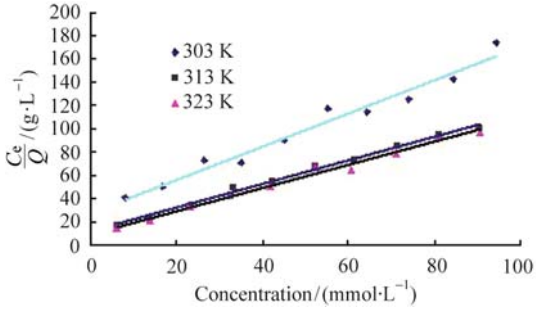

Fig. 7 Langmuir isotherms adsorption model for Cu^{2+} onto RCM at different temperatures

Table 2 Langmuir isotherm parameters for Cu^{2+} with RCM

T/K	Regression equation	Q_s /(mmol·g^{-1})	K_b /(L·$mmol^{-1}$)	R^2
303	$C_e/Q = 27.877 + 1.3849C_e$	0.700	0.051	0.9719
313	$C_e/Q = 11.614 + 1.0075C_e$	0.993	0.087	0.9937
323	$C_e/Q = 9.3765 + 0.9906C_e$	1.009	0.106	0.9908

The data of Table 2 shows that there was marked correlation coefficients in each linear regression equation were over 0.97. It proves that the adsorption behavior of RCM to Cu^{2+} belongs to the Langmuir isotherm adsorption model. The rise of experimental temperature caused an obvious increasing in Q_s. The result shows that increasing the temperature was advantageous to the adsorption behavior of RCM for Cu^{2+} and the adsorption process was concluded to be favorable for adsorption and the adsorption was endothermic. Within the range of experi-

mental concentrations, the characteristics separation coefficient R_L [$R_L = 1/(1 + K_b C_0)$, $0 < R_L < 1$] were 0.662, 0.535 and 0.485 at 303 K, 313 K and 323 K, respectively. It indicated that the adsorption behavior of RCM for Cu^{2+} was the preferential adsorption, the monolayer adsorption model and the energy equivalent adsorption. Furthermore, it indirectly reflected that the stronger interaction of coordination adsorption might play a leading role in the entire adsorption process. The chitosan crystal structure had been weakened for some degree after cross-linking reaction (see the result of XRD) and the effect of hydrogen bonds between hydroxyl groups and amino groups in the RCM decreased, and they were more liable to associate with Cu^{2+} because of their correspondingly increasing activity.

3.3 Adsorption mechanism of Cu^{2+} onto RCM

In general, in the solid sorbent-aqueous solution system, besides van der Waals force that was considered, other interactions, such as hydrogen bonding interaction, hydrophobic interaction, π-π interaction and electrostatic interaction should be considered as well. Among these, the hydrogen bonding interaction had great influence on the adsorption behavior in the non-polar solvent, the hydrophobic interaction played an important role in neutral resin adsorbing non-polar solute in polar solvent, the π-π interaction was the main influence factor of aromatic organic adsorption and the electrostatic interaction had obvious influence on organic ions adsorption. It can be regarded that the adsorption behavior of Cu^{2+} onto RCM was attributed to the hydrogen bonding interaction and the complex formation between Cu^{2+} and amino group of RCM [19, 20]. And the hydrogen bonding interaction can be understood as the generalized Lewis acid and base effect.

3.4 The adsorption thermodynamics behavior of Cu^{2+} onto RCM

3.4.1 The change of adsorption enthalpy

The Clausius-Clapeyron equation is as follows: $\ln C_e = \Delta H/(RT) + K$, in which R is the gas constant ($8.314\ J \cdot K^{-1} \cdot mol^{-1}$), T is the absolute temperature (K), C_e is the adsorption equilibrium concentration ($mmol \cdot L^{-1}$), ΔH is the isosteric adsorption enthalpy ($kJ \cdot mol^{-1}$), K is the adsorption equilibrium constant. The adsorption isostere $\ln C_e$-$1/T$ ($\ln C_e$ given by Langmuir equation) can be obtained by using the adsorption isotherm of Cu^{2+} onto RCM at different temperatures. Fig. 8 was the result and the correlations were good. Therefore, throughout the derivation of the formula, the hypothesis of no correlation between ΔH and T was reasonable in the experimental range of temperature. The slope ($\Delta H/R$) corresponding to adsorption quantity and the isosteric enthalpy ΔH can be calculated by the linear regression method and the results were listed in Table 3. With the increasing Q value, ΔH value increased when Q value was from 0.3 to 0.6 $mmol \cdot g^{-1}$. It was found that the adsorption behavior of Cu^{2+} onto RCM was an endothermic process and the increase of temperature did benefit to the process because of the positive ΔH value.

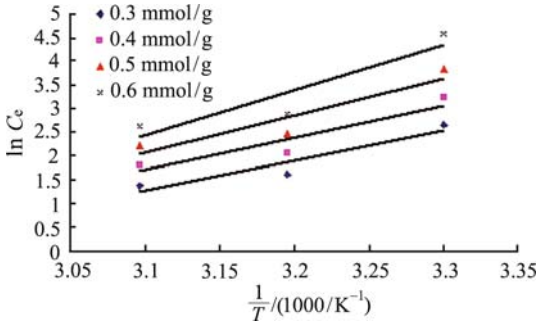

Fig. 8 Determination of enthalpy of adsorption for Cu^{2+} with RCM

The enthalpy change of Cu^{2+} onto RCM mainly included the adsorption heat of $CuSO_4$, the polymer chain force, the energy of destruction chain regularity and the conformational change needed (polymer chain activation energy for short), the desorption heat of solvent water, the dilution heat of solution caused by $CuSO_4$ adsorption, the enthalpies of solvation of the adsorption sites and the solute molecules. The enthalpy change of Cu^{2+} onto RCM usually results from the multiple actions of factors and the positive and negative of enthalpy change was dependent on the contrast result of the total exothermic effect and total endothermic effect. In this experimental system, the total exothermic effect comes from the adsorption heat of $CuSO_4$ and the total endothermic effect was from the

Table 3 Thermodynamic properties of the Cu^{2+} onto RCM

Q/($mmol \cdot g^{-1}$)	H/($kJ \cdot mol^{-1}$)	ΔG/($kJ \cdot mol^{-1}$)			ΔS/($kJ \cdot mol^{-1} \cdot K^{-1}$)		
		303 K	313 K	323 K	303 K	313 K	323 K
0.3	52.170	−7.484	−6.362	−6.036	0.197	0.187	0.180
0.4	57.036	−7.484	−6.362	−6.036	0.213	0.203	0.195
0.5	64.946	−7.484	−6.362	−6.036	0.239	0.228	0.220
0.6	80.553	−7.484	−6.362	−6.036	0.291	0.278	0.268

chitosan chain activation energy. After RCM adsorption of Cu^{2+}, the RCM crystalline might be further decreased, the hydrogen bonds existing in the intramolecular and intermolecular areas might be further destroyed and the chitosan molecular conformation maybe become unstable. All above process would consume a lot of energy. The adsorption quantity of Cu^{2+} onto RCM increased with the rise of the temperature and much more energy might be consumed. As a whole, the adsorption behavior of Cu^{2+} onto RCM was an endothermic process, because the adsorption heat of $CuSO_4$ was less than total endothermic effect. The solvent permutation theory can explain the above result. The metal ions adsorption is an exothermic process. On the contrary, the water molecules desorption is an endothermic process. The total quantity of two independent processes, e.g. the adsorption of adsorbate onto the adsorbent surface and the solvent desorption, would determined the thermodynamic parameters. The whole adsorption process was an endothermic process because one solute molecule was absorbed. Meanwhile, more water molecules were desorbed.

3.4.2 The change of adsorption free energy and adsorption entropy

The adsorption free energy value can be obtained from the Gibbs free energy equation: $\Delta G = -RT\ln K_b$. The adsorption free energy change is the embodiment of adsorption driving force. And the negative adsorption free energy change indicated the adsorption was a spontaneous behavior and the adsorbate was inclined to be absorbed the surface of adsorbent from solution. The ΔG data in Table 3 shows that the adsorption of Cu^{2+} onto RCM was the spontaneous and physical adsorption behavior. The adsorption entropy change can be calculated according to the Gibbs-Helmoltz equation: $\Delta S = (\Delta H - G)/T$. The adsorption free energy change is in the negative ($\Delta G < 0$) because of the spontaneous adsorption process, that is $\Delta H - T\Delta S < 0$. $\Delta S > 0$ and $\Delta S > |\Delta H/T|$ is due to $\Delta H > 0$. Therefore, the adsorption is the entropy increasing process and the adsorption of Cu^{2+} onto RCM is the process of promotion by enthalpy. In the experimental range, the adsorption entropy change was always in the positive. The adsorption process was essential for the exchange process of Cu^{2+} in water solution and adsorbed water molecules on RCM. The negative values of the adsorption Cu^{2+} entropy ΔS indicated the more restricted mobility of Cu^{2+} on the resin surface than it in solution. Furthermore, when Cu^{2+} was adsorbed onto RCM, much more water molecules might be desorbed from RCM and their existing state will be changed, from the closely arranged form on the RCM to the free motion in solution, simultaneously. The desorption entropy change was increased, which was in the positive value. During the replacement process, the displaced water molecules were more than the adsorbed Cu^{2+} ions and the total entropy change in the adsorption process was a positive value because the molar volume of water is far smaller than that of Cu^{2+} ion.

3.4.3 The change of adsorption potential

According to the Polanyi theory, the adsorption potential (E) of the sorbate molecule in the solid surface of an attracting field is the power needed to drive the molecule moving from the current position to the boundless space. Because of the homogeneous body phase concentration, the effect of adsorption force field in the body phase can be neglected compare with the thermal motion effect of body molecule. The adsorption force is zero, that is the interface between the body phase and the adsorption phase is the zero point position. Thus, the above interpretation can be understood that the adsorption potential of the sorbate molecule in the solid surface of attractive field is the power needed to drive the molecule moving from the equipotential surface position in the adsorption phase to the zero point position. The solid-liquid adsorption potential can be expressed in formula: $E = -RT\ln C_e/C_0$. The adsorption potential of Cu^{2+} onto RCM is listed in Table 4.

Table 4 Adsorption potentials of Cu^{2+} onto RCM

C_0/(mmol·L^{-1})	E/(kJ·mol^{-1})		
	303 K	313 K	323 K
10	0.553	1.207	1.413
20	0.459	0.968	1.043
30	0.325	0.654	0.692
40	0.331	0.486	0.570
50	0.265	0.437	0.489
60	0.205	0.359	0.378
70	0.210	0.336	0.387
80	0.209	0.319	0.273
90	0.198	0.297	0.248
100	0.139	0.283	0.216

At an identical measuring temperature, the adsorption potential of Cu^{2+} onto RCM was gradually decreased with the increase of Cu^{2+} concentration. At the same initial Cu^{2+} concentration, the adsorption potential of Cu^{2+} onto RCM was increased with the rise of experimental temperature. When temperature remained a constant, the analysis of adsorption isotherm shows that the adsorption quantity increased with increase of the initial Cu^{2+} concentration. That is to say that during the adsorption process of Cu^{2+} onto RCM, the higher the initial concentration was, the higher the adsorption quantity would be and the higher the adsorption quantity was, the lower the adsorption potential would be. There are mainly two kinds of reasons for the adsorption potential decreased. One was that the adsorption behavior firstly took place on the maximum site of the

surface attractive force due to the heterogeneous surface of RCM. The other was that the surface attractive force decreased with the rise of surface coverage.

4 Conclusions

The preparation of RCM used a reversed phase suspension cross-linking polymerization. The obtained RCM was a type of light yellow spherical resin with smooth surface and the average particle diameter was about 500 μm. The cross-linking reaction happened between glutaraldehyde and amino groups of chitosan due to the appearance of imino group stretch vibration absorption in FTIR spectra. This result was proven by the XRD diffraction spectra of the Form I diffraction peak disappearance and the Form II diffraction peak relative intensity decreased and the DSC curves of the endothermic peak temperature being more than chitosan and the exothermic peak temperature being less than chitosan. The results show that the adsorption of Cu^{2+} onto RCM obeyed the Langmuir isotherm and the adsorption was a spontaneous increasing enthalpy and entropy driving process.

References

1. Rhazi M, Desbrières J, Tolaimate A, Rinaudo M, Vottero P, Alagui A, El Meray M. Influence of the nature of the metal ions on the complexation with chitosan. Application to the treatment of liquid waste.European Polymer Journal, 2002, 38: 1523–1530
2. Sun S L, Wang A Q. Adsorption properties and mechanism of cross-linked carboxymethyl-chitosan resin with Zn (II) as template ion. Reactive & Functional Polymers, 2006, 66: 819–826
3. Ramnani S P, Sabharwal S. Adsorption behavior of Cr (VI) onto radiation crosslinked chitosan and its possible application for the treatment of wastewater containing Cr (VI). Reactive & Functional Polymers, 2006, 66: 902–909
4. Shan B T, Zhou A H, Liang S K, Wang X L. Composition and characteristics of a bioflocculant produced by a *Sphingobacterium sp*.. Periodical of Ocean University of China, 2006, 36(5): 804–808 (in Chinese)
5. Wang Y D, Gao M C, She Z L, Gu Y Y. Study on the decolorization kinetics of reactive red K-2BP wastewater by spongy iron. Periodical of Ocean University of China, 2006, 36(suppl): 137–140 (in Chinese)
6. Zhang Y Y, Ma Q M. Adsorbent prepared from modified chitosan derivatives and study of its adsorption behavior. Periodical of Ocean University of China, 2006, 36(suppl): 153–156 (in Chinese)
7. Wang D F, Yu L N, Su L, Zhang Y W, Wang C H. Resins of chitosan - Ce^{4+} complexes application in apple juice production. Chinese Rare Earths, 2006, 27(1): 11–14 (in Chinese)
8. Su L, Wang D F, Yu L N, Geng J, Li L, Sun J P. Application of chitosan/ Ce^{4+} particles in the production of pullucid fruit juice. Food and Fermentation Industries, 2006, 32(1): 141–143 (in Chinese)
9. Yu L N, Wang D F, Li H Y, Su L, Wang J L. Hydrolysis activities of resins of complexes made from polysaccharides and Ce^{4+}. Journal of Rare Earths, 2006, 24 (spec): 125–129 (in Chinese)
10. Yu Y H, Sun Y, He B L. Preparation and characterization of crosslinked chitosan resin. Transactions of Tianjin University, 2000, 33(1): 113–117 (in Chinese)
11. Wang D F, Yu L N, Su L, Sun L P. The preparation technology on one kind of multi-functional rare earth polysaccharide microspheres. Chinese invention patent (ZL 200510042228.8), 2005-03-25 (in Chinese)
12. Kosaraju S L, D'ath L , Lawrence A. Preparation and characterisation of chitosan microspheres for antioxidant delivery. Carbohydrate Polymers, 2006, 64: 163–167
13. Zong Z, Kimura Y, Takahashi M, Yamane H. Characterization of chemical and solid state structures of acylated chitosans. Polymer, 2000, 41: 899–906
14. Tang W J, Wang C X, Chen D H. Kinetic studies on the pyrolysis of chitin and chitosan. Polymer Degradation and Stability, 2005, 87: 389–394
15. Neto C G T, Giacometti J A, Job A E, Ferreira F C, Fonseca J L C, Pereira M R. Thermal analysis of chitosan based networks. Carbohydrate Polymers, 2005, 62: 97–103
16. Fujiwara K, Ramesh A, Maki T, Hasegawa H, Ueda K. Adsorption of platinum (IV), palladium (II) and gold (III) from aqueous solutions onto L-lysine modified crosslinked chitosan resin. Journal of Hazardous Materials, 2006, 49: 1–12
17. Ngah W S W, Fatinathan S. Chitosan flakes and chitosan-GLA beads for adsorption of *p*-nitrophenol in aqueous solution. Colloids and Surfaces A: Physicochem Eng Aspects, 2006, 277: 214–222
18. Chang Y C, Chen D H. Preparation and adsorption properties of monodisperse chitosan-bound Fe3O4 magnetic nanoparticles for removal of Cu (II) ions. Journal of Colloid and Interface Science, 2005, 283: 446–451
19. Guzman J, Saucedo I, Revilla J, Navarro R, Guibal E. Copper sorption by chitosan in the presence of citrate ions: influence of metal speciation on sorption mechanism and uptake capacities. International Journal of Biological Macromolecules, 2003, 33: 57–65
20. Li N, Bai R. Copper adsorption on chitosan-cellulose hydrogel beads: behaviors and mechanisms. Separation and Purification Technology, 2005, 42: 237–247